



ELSEVIER

Thermochimica Acta 260 (1995) 115–124

---

---

thermochimica  
acta

---

---

## Thermal decomposition of ammonium vanadyl oxalate supported on various oxides

X.S. Li \*, L.Y. Chen, C.Y. Xie, Y.F. Miao, D.M. Li, Q. Xin

*State Key Laboratory of Catalysis, Dalian Institute of Chemical Physics, Chinese Academy of Sciences,  
Dalian 116023, China*

Received 14 January 1995; accepted 3 February 1995

---

### Abstract

The thermal decomposition of ammonium vanadyl oxalate supported on  $\text{La}_2\text{O}_3$ ,  $\text{MgO}$ ,  $\text{SiO}_2$ ,  $\text{Al}_2\text{O}_3$ ,  $\text{ZrO}_2$ ,  $\text{TiO}_2$ , SAPO-5, and ZSM-5 oxides in a dynamic atmosphere of dry air was compared by thermal gravimetric analysis (TG) and differential thermal analysis (DTA). The calcined catalysts were characterized by X-ray diffractometry (XRD). The TG and DTA results demonstrate that the surface acid–base properties of the oxides play a significant role in the decomposition behaviour of the supported ammonium vanadyl oxalate, i.e. the basic oxides exhibit an endothermic effect and the acidic oxides show an exothermic effect. Two mechanisms are suggested for thermal decomposition of ammonium vanadyl oxalate on basic and acidic oxides, respectively. After transformation of the vanadia on the ammonium vanadyl oxalate to vanadia, subsequent rearrangement of the vanadia on the surface of the supports was also observed. During the thermal treatment or calcination in air, solid state reactions of vanadia with the surface of oxides such as  $\text{La}_2\text{O}_3$ ,  $\text{ZrO}_2$  and  $\text{TiO}_2$  took place to form new phases.

*Keywords:* Oxide-supported ammonium vanadyl oxalate; Thermal decomposition

---

### 1. Introduction

It is well known that vanadium-based catalysts are used extensively in heterogeneous catalysis, including selective oxidation and de- $\text{NO}_x$  reactions [1, 2]. In recent years, much attention has been focused on oxide-supported vanadium systems due to their advantages of high activity, selectivity and good stability as compared with pure  $\text{V}_2\text{O}_5$  or phosphorus-promoted  $\text{V}_2\text{O}_5$  catalysts [3–9]. Different carriers show distinct

---

\* Corresponding author.

influences on the activity and selectivity of the tested reactions, as reported by Kijenski et al. [5] and Sharma et al. [6]. In most cases, supported vanadium catalysts are prepared by impregnation methods. Ammonium metavanadate and ammonium vanadyl oxalate are usually used as the precursors. The standard procedure is: impregnation of oxide with the solution of vanadate compound; drying at moderate temperature to remove excess solvent; calcination to transfer the precursor to active vanadia. From a practical point of view, a knowledge of the decomposition mechanism of the precursors under air atmosphere is fundamental to the selective formation of vanadia with specific characteristics such as texture, structure and its interaction with the support. However, literature information in this area is very sparse. Therefore, the present study focused on the investigation of the thermal decomposition of ammonium vanadyl oxalate supported on various oxides made by the impregnation method.

## 2. Experimental

### 2.1. Materials

The supports used in this paper were  $\text{La}_2\text{O}_3$ ,  $\text{MgO}$ ,  $\text{Al}_2\text{O}_3$ ,  $\text{SiO}_2$ ,  $\text{TiO}_2$ ,  $\text{ZrO}_2$  and two kinds of zeolites, namely silicoaluminophosphate (SAPO-5) and aluminosilicate (ZSM-5) [10, 11]. The supported vanadia catalysts were prepared by the impregnation method. The impregnating solution was obtained by dissolving  $\text{NH}_4\text{VO}_3$  in aqueous oxalic acid solution at 353 K. The molar ratio of  $\text{NH}_4\text{VO}_3$  to oxalic acid was 1:2. The resulting deep blue solution contained the compound  $(\text{NH}_4)_2[\text{VO}(\text{C}_2\text{O}_4)_2]$ , the vanadium being in the 4+ oxidation state [1]. After impregnation, the excess water was removed by evaporation at 373 K, and then the solids were dried at 393 K for 20 h. These solids were kept dry and used as precursors for further thermal analysis. The calcined catalysts were obtained by heating the precursors at 873 K for 8 h in air. The nominal weight percentage of vanadia in all the supported catalysts is 10%.

### 2.2. Methods

BET surface area measurements were performed with a Micromeritics ASAP-2000 using nitrogen as an absorbant after the calcined samples were degassed in vacuum at 623 K for at least 4 h.

The thermal analysis of the catalyst precursors without calcination was carried out using Perkin-Elmer DTA-1700 and Perkin-Elmer TGS-2 instruments coupled to a Perkin-Elmer 3600 data station in flowing dry air at a heating rate of  $10 \text{ K min}^{-1}$ .

X-ray diffraction (XRD) analysis was performed with a Regaku Rotaflex (Ru-200B) instrument using Ni-filtered  $\text{CuK}\alpha_1$  radiation and operated at 40 kV and 50 mA.

## 3. Results and discussion

The surface areas, pore volumes and XRD characteristics of the carriers and the calcined supported vanadia catalysts are summarized in Table 1. It is well known that

Table 1  
Surface areas, pore volumes and XRD determination of the carriers and the calcined supported vanadia catalysts

Catalysts	$S_{\text{BET}}/(\text{m}^2 \text{g}^{-1})$	$V_p/(\text{cm}^3 \text{g}^{-1})$	XRD
$\text{La}_2\text{O}_3$	9.4	0.012	
$\text{V}/\text{La}_2\text{O}_3$	8.6	0.005	New unidentified phase
$\text{MgO}$	31	0.021	
$\text{V}/\text{MgO}$	167	0.442	No $\text{V}_2\text{O}_5$ phase
$\text{SiO}_2$	289	0.282	
$\text{V}/\text{SiO}_2$	137	0.123	$\text{V}_2\text{O}_5$ phase
$\text{Al}_2\text{O}_3$	74	0.131	
$\text{V}/\text{Al}_2\text{O}_3$	59	0.053	No $\text{V}_2\text{O}_5$ phase
$\text{ZrO}_2$	7.7	0.005	
$\text{V}/\text{ZrO}_2$	10.3	0.006	$\text{V}_2\text{O}_5$ phase
$\text{TiO}_2$	3.8	0.001	
$\text{V}/\text{TiO}_2$	4.6	0.000	$\text{V}_2\text{O}_5$ phase
SAPO-5	92	0.104	
$\text{V}/\text{SAPO-5}$	105	0.040	No $\text{V}_2\text{O}_5$ phase
ZSM-5	318	0.141	
$\text{V}/\text{ZSM-5}$	263	0.100	No $\text{V}_2\text{O}_5$ phase

$\text{La}_2\text{O}_3$  and  $\text{MgO}$  are basic oxides. When ammonium vanadyl oxalate was supported on  $\text{La}_2\text{O}_3$  and  $\text{MgO}$ , similar decomposition reactions were observed with one main endothermic peak at 670–710 K as seen in Fig. 1. From the TG curves of these two samples, it is seen that there was a significant weight loss resulting from the decomposition of ammonium vanadyl oxalate in the temperature range 553–823 K. Furthermore, subtle differences were found in the DTA curves of the two catalyst precursors. The  $(\text{NH}_4)_2[\text{VO}(\text{C}_2\text{O}_2)_2]/\text{MgO}$  showed only one main endothermic effect at 700 K. In contrast, the  $(\text{NH}_4)_2[\text{VO}(\text{C}_2\text{O}_2)_2]/\text{La}_2\text{O}_3$  showed a small endothermic peak at 803 K as well as the main endothermic peak at 678 K. Comparing the DTA results with those of the TG curves, the main endothermic effects on both  $(\text{NH}_4)_2[\text{VO}(\text{C}_2\text{O}_2)_2]/\text{La}_2\text{O}_3$  and  $(\text{NH}_4)_2[\text{VO}(\text{C}_2\text{O}_2)_2]/\text{MgO}$  samples can be assigned to the decomposition of ammonium vanadyl oxalate. After calcination of the above two samples, XRD patterns show no diffraction peak corresponding to the  $\text{V}_2\text{O}_5$  phase. However, some new diffraction peaks appeared on the calcined  $\text{V}/\text{La}_2\text{O}_3$  sample indicating that solid state reaction of the vanadia and the surface of  $\text{La}_2\text{O}_3$  occurred during the thermal treatment (Fig. 2). The peak at 803 K in the DTA curve of  $(\text{NH}_4)_2[\text{VO}(\text{C}_2\text{O}_2)_2]/\text{La}_2\text{O}_3$  probably corresponds to this reaction. Unfortunately the new species formed on the calcined  $\text{V}/\text{La}_2\text{O}_3$  sample has not been identified in the present study.

The TG and DTA curves of the decomposition of ammonium vanadyl oxalate supported on  $\text{Al}_2\text{O}_3$  and  $\text{SiO}_2$  are shown in Fig. 3. For the  $(\text{NH}_4)_2[\text{VO}(\text{C}_2\text{O}_2)_2]/\text{Al}_2\text{O}_3$  sample, an exothermic peak appears at 594 K and is followed by a flat exothermic peak in the temperature range 673–863 K. The TG curve shows that the weight loss ends at about 633 K corresponding with the complete decomposition of ammonium vanadyl

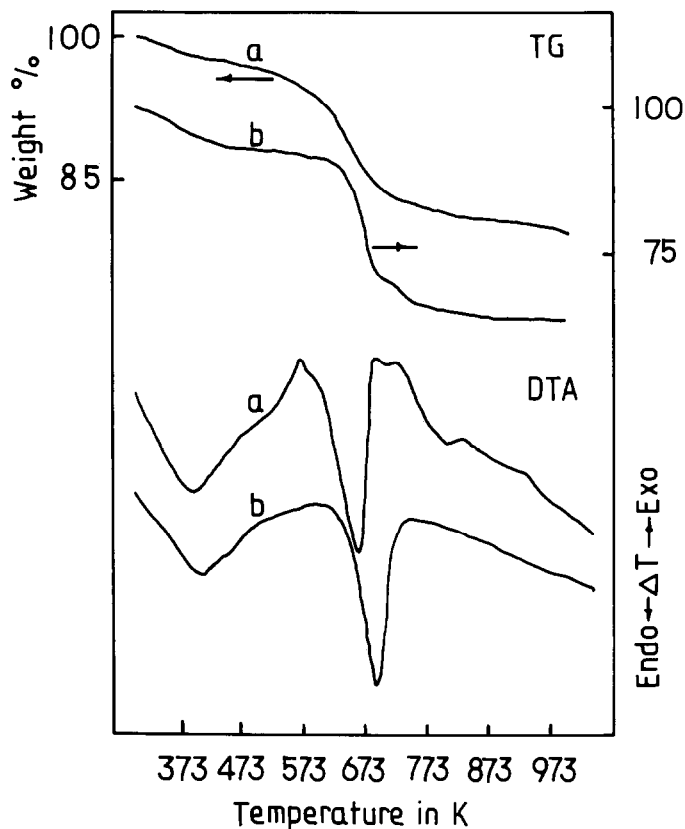


Fig. 1. DTA and TG curves of ammonium vanadyl oxalate supported on (a)  $\text{La}_2\text{O}_3$  and (b)  $\text{MgO}$  oxides.

oxalate before this temperature. Therefore, it is deduced that the flat exothermic peak is due to redispersion of the vanadia on the surface of  $\text{Al}_2\text{O}_3$  [9], which means that a strong interaction occurs between the vanadia and the surface of  $\text{Al}_2\text{O}_3$ . No  $\text{V}_2\text{O}_5$  phase was seen in the XRD pattern of the calcined  $\text{V}/\text{Al}_2\text{O}_3$ . However, different results were observed on decomposition of ammonium vanadyl oxalate supported on  $\text{SiO}_2$ . The DTA curve of  $(\text{NH}_4)_2[\text{VO}(\text{C}_2\text{O}_4)_2]/\text{SiO}_2$  gives an exothermic peak at 598 K as well as the main endothermic effect at 379 K, indicating the end of the weight loss before 613 K in the TG curve. In addition, the diffraction peaks corresponding to  $\text{V}_2\text{O}_5$  phase were observed in the XRD pattern of the calcined  $\text{V}/\text{SiO}_2$  catalyst. Though  $\text{SiO}_2$  has a higher surface area than  $\text{Al}_2\text{O}_3$ , as given in Table 1, the presence of  $\text{V}_2\text{O}_5$  phase on the calcined  $\text{V}/\text{SiO}_2$  could be contributing to weak interactions between the vanadia and  $\text{SiO}_2$ , giving rise to the formation of the  $\text{V}_2\text{O}_5$  phase on the surface of  $\text{SiO}_2$ .

The thermal decomposition of ammonium vanadyl oxalate supported on  $\text{TiO}_2$  and  $\text{ZrO}_2$  is shown in Fig. 4. The two samples have similar decomposition characteristics, showing one large exothermic peak with an exothermic shoulder. For the

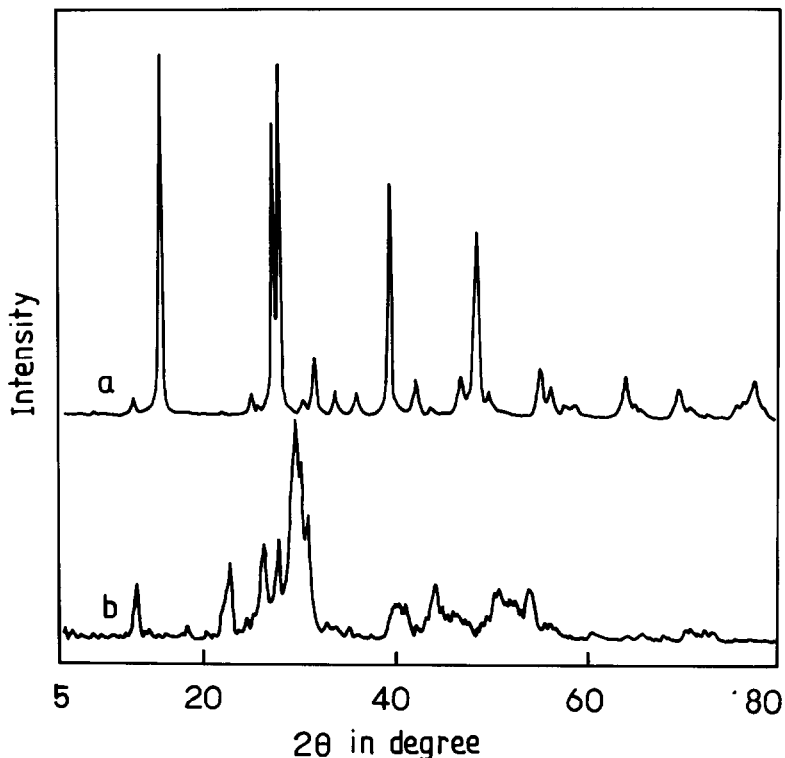


Fig. 2. XRD patterns of (a)  $\text{La}_2\text{O}_3$  and (b) the calcined  $\text{V}/\text{La}_2\text{O}_3$  catalyst.

$(\text{NH}_4)_2[\text{VO}(\text{C}_2\text{O}_2)_2]/\text{TiO}_2$  sample, the main peak was observed at 592 K, and the shoulder at 673 K. For the  $(\text{NH}_4)_2[\text{VO}(\text{C}_2\text{O}_2)_2]/\text{ZrO}_2$  sample, the main peak was at 606 K and the shoulder peak at 633 K. In addition, both samples showed clear endothermic peaks at 827 and 935 K, respectively, which were more intense for  $(\text{NH}_4)_2[\text{VO}(\text{C}_2\text{O}_2)_2]/\text{TiO}_2$  than for  $(\text{NH}_4)_2[\text{VO}(\text{C}_2\text{O}_2)_2]/\text{ZrO}_2$ . The DTA curves of the pure carriers show no effects at temperature above 473 K (Fig. 4, curves (c) and (d)). The TG curves of the two samples show that the final temperature of weight loss is below 623 K; therefore the shoulder peaks and endothermic effects that appear at higher temperature on the DTA curves cannot be attributed to gas evolution from the thermal decomposition of the samples. Furthermore, XRD results of their calcined samples showed that the  $\text{V}_2\text{O}_5$  phase was produced on the surface. The appearance of  $\text{V}_2\text{O}_5$  is probably due to the low surface areas of  $\text{TiO}_2$  and  $\text{ZrO}_2$ . Salch et al. [7] have also studied in detail the decomposition of ammonium vanadyl oxalate supported on  $\text{TiO}_2$  and they found that ammonium vanadyl oxalate started to decompose to form a complete monolayer of surface vanadia species coordinated to the titania support and  $\text{V}_2\text{O}_5$  crystallites at an intermediate calcination temperature, 623–850 K. When the temperature was increased to above 850 K, the supported vanadia phase reacted with  $\text{TiO}_2$  to yield  $\text{V}_x\text{Ti}_{1-x}\text{O}_2$ . Accordingly, we tend to regard the main exothermic effect as

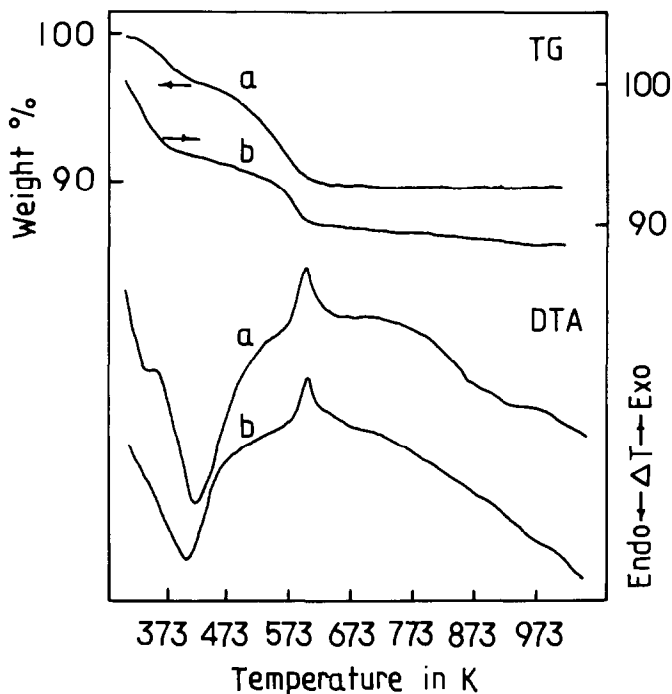


Fig. 3. DTA and TG curves of ammonium vanadyl oxalate supported on (a)  $\text{Al}_2\text{O}_3$  and (b)  $\text{SiO}_2$  oxides.

being due to the decomposition of the ammonium vanadyl oxalate; the shoulder is due to crystallization of vanadia on the surface of  $\text{TiO}_2$  and  $\text{ZrO}_2$  to form  $\text{V}_2\text{O}_5$  phase, and the endothermic effect at high temperature can be assigned to the solid reaction of vanadia with the supports to form new surface species. These results demonstrate that strong interaction between vanadia and the  $\text{TiO}_2$  and  $\text{ZrO}_2$  supports occurred in both systems.

Two kinds of zeolites, SAPO-5 and ZSM-5, were used. Ammonium vanadyl oxalate supported on these two zeolites exhibited different behaviour as shown in Fig. 5. On the  $(\text{NH}_4)_2[\text{VO}(\text{C}_2\text{O}_2)_2]/\text{SAPO-5}$  sample, the TG curve shows constant weight at temperatures above 613 K. In the DTA curve, one small exothermic peak is seen at 598 K with a shoulder at 573 K, and it is followed by a very flat peak at 623 K. In contrast, the thermal decomposition of ammonium vanadyl oxalate supported on ZSM-5 shows an exothermic phenomenon in a wide temperature range of 533–743 K on the DTA curve. The maximum peak is at 693 K with a flat shoulder peak at 610 K. It is worth noting that its TG curve shows a different trend from the result obtained for  $(\text{NH}_4)_2[\text{VO}(\text{C}_2\text{O}_2)_2]/\text{SAPO-5}$ , i.e. its weight loss gradually reached a plateau at a higher temperature of 703 K. From a comparison of the DTA and TG curves of the  $(\text{NH}_4)_2[\text{VO}(\text{C}_2\text{O}_2)_2]/\text{ZSM-5}$  sample, the flat exothermic peak in the DTA could be ascribed to decomposition of ammonium vanadyl oxalate. To understand this specific characteristic of the  $(\text{NH}_4)_2[\text{VO}(\text{C}_2\text{O}_2)_2]/\text{ZSM-5}$  sample, the pore distributions of

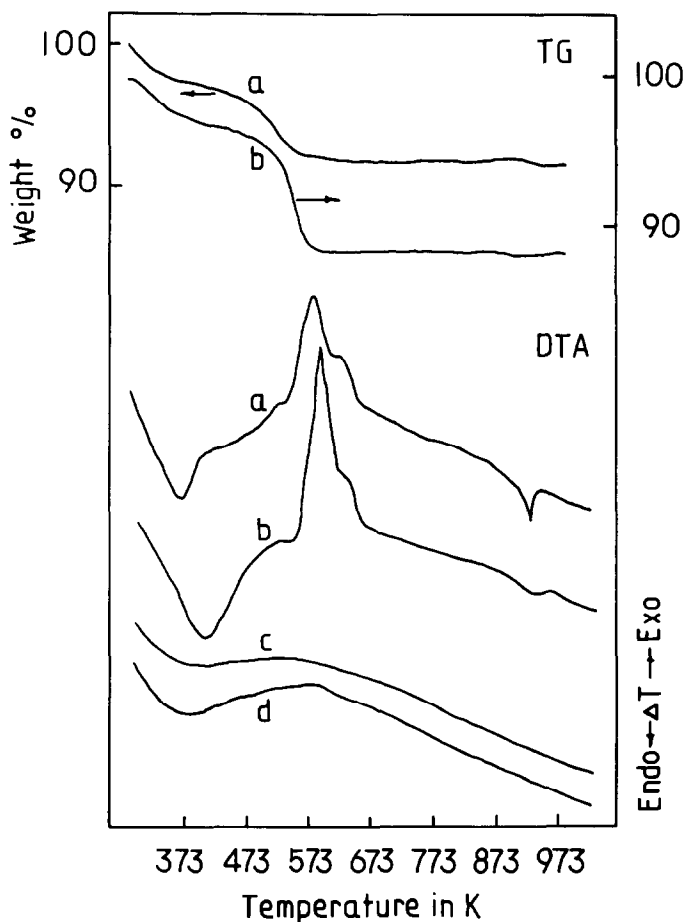


Fig. 4. DTA and TG curves of ammonium vanadyl oxalate supported on (a)  $\text{TiO}_2$  and (b)  $\text{ZrO}_2$  oxides; (c) and (d) are the pure carriers of  $\text{TiO}_2$  and  $\text{ZrO}_2$ , respectively.

ZSM-5 and the calcined V/ZSM-5 catalyst are compared in Fig. 6. ZSM-5 and V/ZSM-5 showed a similar pore distribution except that the cumulative pore volume of the former was higher than the latter. This indicates that at least a fraction of  $\text{NH}_4^+$  and/or vanadyl oxalate ions diffuse into the inner pore and are adsorbed on the wall of the pore of the carrier during the impregnation. This is probably a major reason for delaying the thermal decomposition process. Further XRD measurement did not give any diffraction peaks corresponding to  $\text{V}_2\text{O}_5$  phase on either of the calcined samples.

The large differences observed in the thermal decomposition of ammonium vanadyl oxalate supported on basic and acidic oxides need to be interpreted. During impregnation and thermal processing,  $\text{NH}_3$  can be formed and adsorbed on the acidic sites [2,12]. Undoubtedly, the desorption energy of  $\text{NH}_3$  or  $\text{NH}_4^+$  adsorbed on the acidic

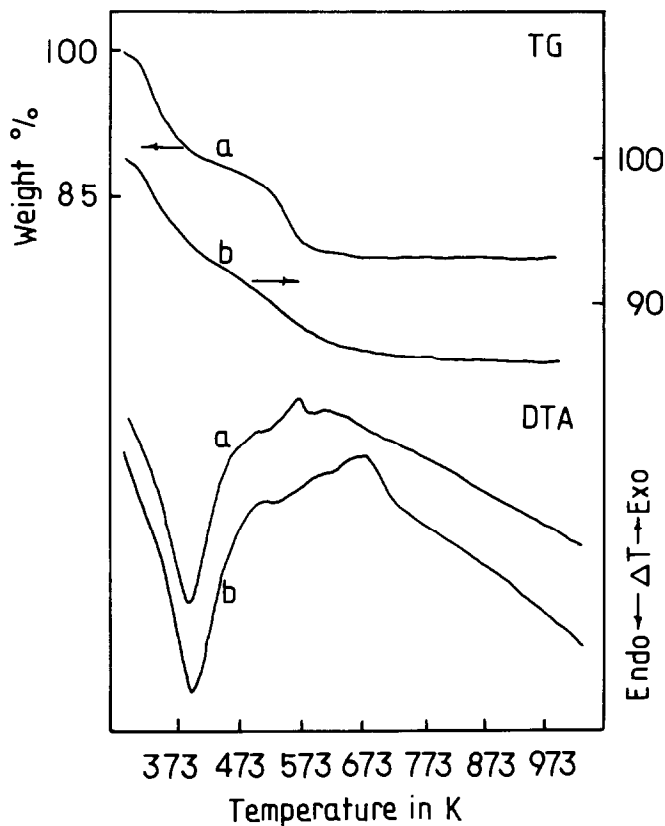
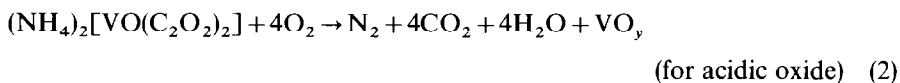
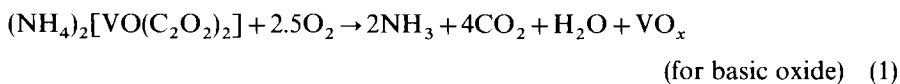


Fig. 5. DTA and TG curves of ammonium vanadyl oxalate supported on (a) SAPO-5 and (b) ZSM-5 zeolites.

sites is so high that its desorption will occur at higher temperatures. The long release time makes it possible for it to react with oxygen to form more water [13], and results in strong exothermic effects which compensates the endothermic effect of the decomposition of the vanadyl oxalate. In contrast, on the basic oxide support, the  $\text{NH}_4^+$  ions and/or the  $\text{NH}_3$  desorb easily and rarely take part in the reaction with oxygen. Accordingly, the total decomposition mechanisms of ammonium vanadyl oxalate supported on basic and acidic oxides could be visualized as follows



Oxidation of  $\text{V}^{4+}$  is expected to occur in the thermal process, which has been recognized to cause rearrangement of the vanadia formed from the decomposition of



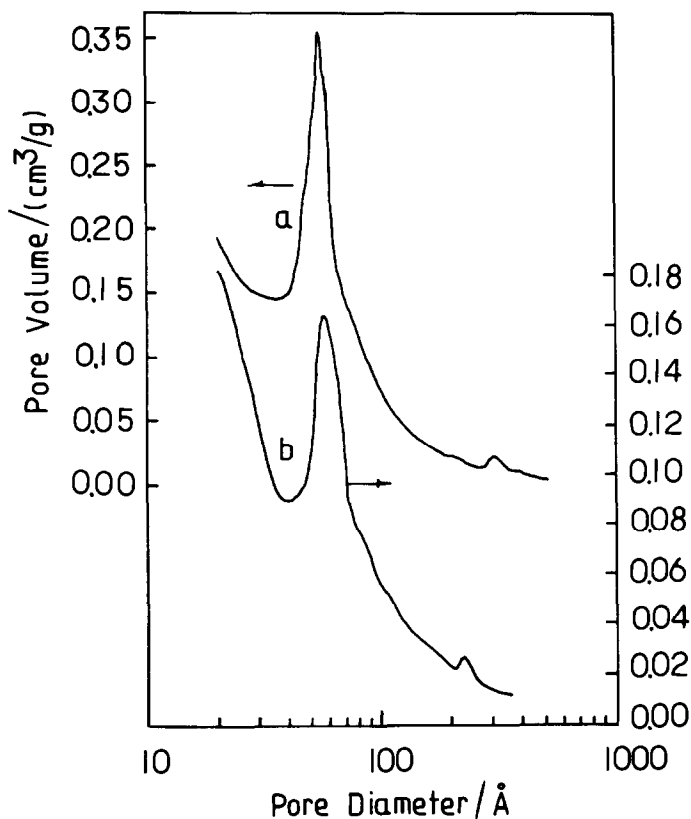


Fig. 6. Pore distribution of (a) ZSM-5 and (b) the calcined V/ZSM-5 catalyst.

ammonium vanadyl oxalate [9]. Since the formation of the  $V_2O_5$  phase was observed for the  $TiO_2$  and  $ZrO_2$  samples with low surface areas as well as for the  $SiO_2$  phase with high surface area, it could be concluded that the surface area is not the sole factor in forming the  $V_2O_5$  phase. The formation of the  $V_2O_5$  phase can be attributed to the interconnection of the vanadia by V–O–V bonds during the decomposition of the vanadyl oxalate as suggested by Kijenski et al. [5]. The species in V–O–V form is probably a precursor of the  $V_2O_5$  phase. After decomposition of the oxalate, rearrangement of the vanadia to produce the  $V_2O_5$  phase will also be decided by the interaction of the vanadia with the carrier. The stronger the interaction, the more highly the vanadia is dispersed on the carrier which decreases the possibility of the formation of  $V_2O_5$  phase. The reverse is the case for weak interactions, e.g. for ammonium vanadyl oxalate supported on  $SiO_2$ . Although the vanadia supported on  $TiO_2$  and  $ZrO_2$  exhibits strong interaction with the carrier, second and multiple layer vanadium can be formed due to the low surface areas of the carriers, so that in these cases the  $V_2O_5$  phase can also easily be formed on top of the monolayer, as detected by XRD.

#### 4. Conclusions

The thermal decomposition of ammonium vanadyl oxalate supported on various oxides proceeded in two steps: decomposition, and rearrangement of vanadia species on the surface of the supports. The surface chemical features of the oxides have an important effect on the decomposition. The thermal decomposition of ammonium vanadyl oxalate exhibits a strong endothermic effect on basic oxides and, in contrast, an exothermic effect on acidic oxides. Subsequent formation of the  $V_2O_5$  phase depends on the interaction of the vanadia species with the supports. Evident surface solid reactions between the vanadia formed and the surface of the carriers were observed on V/La<sub>2</sub>O<sub>3</sub>, V/TiO<sub>2</sub> and V/ZrO<sub>2</sub> catalyst systems to form some new phases. On V/ZSM-5 catalyst, ammonium vanadyl oxalate can diffuse into the inner pores of the carrier, which delays the process of decomposition.

#### Acknowledgements

We thank Prof. Z.C. Tan for helpful discussion. The financial support given by the Science and Technology Committee of Liaoning Province (China) is gratefully acknowledged.

#### References

- [1] G.C. Bond and S.F. Tahir, *Appl. Catal.*, 71 (1991) 1.
- [2] R.A. Rajadhyaksha and H. Knozinger, *Appl. Catal.*, 51 (1989) 81.
- [3] P. Malet, A. Munoz-Paez, C. Martin and V. Rives, *J. Catal.*, 134 (1992) 47.
- [4] A.J. van Hengstum, J.G. van Ommen, H. Bosch and P.J. Gellings, *Appl. Catal.*, 5 (1983) 207.
- [5] J. Kijenski, A. Baiker, M. Gliski, P. Dollenmeier and A. Wokaun, *J. Catal.*, 101 (1986) 1.
- [6] V.K. Sharma, A. Wokaun and A. Baiker, *J. Phys. Chem.*, 90 (1986) 2715.
- [7] R.Y. Salch, I.E. Wachs, S.S. Chan and C.C. Chersich, *J. Catal.*, 98 (1986) 102.
- [8] J.G. Eon, R. Olier and J.C. Volta, *J. Catal.*, 145 (1994) 318.
- [9] P.J. Anderson and H.H. Kung, *J. Phys. Chem.*, 96 (1992) 3114.
- [10] *Zeolite*, 12 (1992) 138.
- [11] B.M. Lok, C.A. Messina, R.L. Patton, R.T. Gajek, T.R. Cannan and E.M. Flanigen, *J. Am. Chem. Soc.*, 106 (1984) 6092.
- [12] Z. Sobalik, R. Kozloski and J. Haber, *J. Catal.*, 127 (1991) 665.
- [13] G. Dell'Agli, S.M. Grippo and G. Mascolo, *Thermochim. Acta*, 227 (1993) 197.